Biosensors and Bioelectronics 24 (2009) 1189–1194

Contents lists available at ScienceDirect

Biosensors and Bioelectronics

journal homepage: www.elsevier.com/locate/bios

On-chip detection of protein glycosylation based on energy transfer between nanoparticles

Young-Pil Kim, Sunyoung Park, Eunkeu Oh, Young-Hee Oh, Hak-Sung Kim*

Department of Biological Sciences, Korea Advanced Institute of Science and Technology (KAIST), 373-1, Guseong-dong, Yuseong-gu, Daejeon 305-701, Republic of Korea

ARTICLE INFO

Article history:
Received 11 March 2008
Received in revised form 3 July 2008
Accepted 4 July 2008
Available online 18 July 2008

Keywords:
Glycosylation
Glycoprotein
Energy transfer
Gold nanoparticle
Quantum dot
Biochip

ABSTRACT

We describe a chip-based method to detect protein glycosylation based on the energy transfer between quantum dots (QDs) and gold nanoparticles (AuNPs). Our assay system relies on modulations in the energy transfer between the nanoparticles on a surface. The photoluminescence (PL) of lectin-coated QDs (energy donor) immobilized on a glass slide is quenched by carbohydrate-coated AuNPs (energy acceptor), and the presence of the glycoprotein causes the increase of the PL of QDs. As a proof-of-concept, Concanavalin A-coated QDs (ConA-QDs) and dextran-coated AuNPs (Dex-AuNPs) were used to detect the mannosylated proteins. As a result, the PL intensity of QDs was found to be linearly correlated with the concentration and the number of glycan moiety of the glycoprotein. We anticipated that our simple assay system will find applications for the analysis of glycoproteins with high selectivity and sensitivity in a high-throughput manner.

1. Introduction

Glycoproteins are naturally occurring saccharide-conjugated proteins that play an important role in many biological events, including the immune response, cellular proliferation, and the progression of tumor cells (Bertozzi and Kiessling, 2001; Ohtsubo and Marth, 2006). Elucidation of the specific interactions and properties of glycoproteins with their virtually unlimited structural diversity is essential for understanding fundamental biological processes in living cells, and can provide effective means for developing novel therapeutics and improved diagnostic systems. To date, a range of techniques such as affinity chromatography (Caron et al., 1998), capillary electrophoresis–mass spectrometry (Zamfir and Peter-Katalinic, 2004), and surface plasmon resonance (SPR) (Kim et al., 2007a; Mann et al., 1998) have been successfully employed to selectively analyse the degree of glycosylation in proteins. However, most of the above methods, which typically involve the use of lectins having a relatively low affinity level (i.e., dissociation constant $\approx 10^{-3}$ to 10^{-6} M), are rather laborious and time-consuming. As an alternative, carbohydrate- or lectin-based microarrays have also been examined as potential platforms for the high-throughput analysis of glycoproteins using fluorescently labeled probes (Chen et al., 2007; Manimala et al., 2006; Pilobello et al., 2005). A major disadvantage of microarray-based approaches, however, is that several cycles of affinity binding and washing steps using labeled molecules such as lectins, antibodies or glycoproteins are needed prior to the analysis. In addition, the organic fluorophores typically used in such methods are highly susceptible to photobleaching, and thus a significant level of background noise is often generated.

Recently, Förster resonance energy transfer (FRET), a type of non-radiative energy transfer mechanism that can occur between a suitably matched acceptor and donor pair (Sapsford et al., 2006), has attracted much attention because of its intrinsically high level of sensitivity to nanoscale proximity changes. Quantum dot (QD)-based FRET systems are of particular interest owing to several distinctive optical properties, including high quantum yield, capability for multiplexed analyses using a single excitation wavelength, and high resistance to chemical and photodegradation (Clapp et al., 2004; Medintz et al., 2003). In addition, it has been reported that the combined use of QDs and gold nanoparticles (AuNPs) in a FRET-based system can be a highly effective means for detecting biomolecular interactions in solution (Oh et al., 2005, 2006; Zhang et al., 2008). Nonetheless, little attention has been paid to the chip-based energy transfer systems, which could have great potential for implementation in platforms for the high-throughput analysis of biomolecules.

Here we describe a chip-based system for the detection of protein glycosylation using FRET-based energy transfer between QDs and AuNPs. Basic principle relies on modulation in the energy transfer efficiency between the lectin-modified QDs and

* Corresponding author. Tel.: +82 42 869 2616; fax: +82 42 869 2610.
E-mail address: hskim76@kaist.ac.kr (H.-S. Kim).

0956-5663/$ – see front matter © 2008 Elsevier B.V. All rights reserved.
doi:10.1016/j.bios.2008.07.012

carbohydrate-conjugated AuNPs by glycoproteins. In contrast to solution-based systems, a chip-based format enables more reliable analyses with no aggregation of the nanoparticles, requiring a much smaller amount of reagents (Kim et al., 2007b, 2008). Moreover, the energy transfer mechanism taking place between the nanoparticles allows the development of a simple and highly sensitive method for the detection of glycoproteins.

2. Materials and methods

2.1. Materials

Concanavalin A (ConA) and 2-iminothiolane hydrochloride (98%) were purchased from Sigma. Amino-dextran (MW 10000), Alexa Fluor 647-labeled dextran and carboxyl QDs (Qdot® 525 and Qdot® 605) were from Invitrogen. An amine-reactive hydrogel-coated glass slide (Nexterion™ Slide H) was obtained from Schott Nexterion (Germany). α-D-Mannopyranosyl phenyl isothiocyanate (MPI) and β-D-galactopyranosyl phenyl isothiocyanate (GPI) were purchased from Sigma. Methoxypoly(ethylene glycol)-amine (*m*PEG-NH_2, MW 5000) and methoxypoly(ethylene glycol)-thiol (*m*PEG-SH, MW 5000) were from Nektar Inc. 1-Ethyl-3-[3-dimethylaminopropyl] carbodiimide (EDC) was purchased from Pierce. Hydrogen tetrachloroaurate(III) trihydrate (99.9% $HAuCl_4 \cdot 3H_2O$), sodium citrate dihydrate (99.9%, 2-hydroxy-1,2,3-propanetricarboxylic acid trisodium salt, $C_6H_5Na_3O_7 \cdot 2H_2O$), sodium borohydride (99%, $NaBH_4$), and a chambered silicon coverslip (50 wells, 3 mm × 1 mm, sterile) were purchased from Sigma–Aldrich.

2.2. Synthesis of Dex-AuNPs

AuNPs with an average size of 5 nm (Ted Pella, Inc.) were used at a concentration of 83 nM (5×10^{13} particles mL^{-1}). Dextran-conjugated AuNPs were synthesized by mixing a thiolated dextran and the AuNPs. Thiolated dextran was synthesized by covalent modification of the amino groups of dextran with 2-iminothiolane. In this procedure, a solution of 1 mM amino-dextran (250 μL in distilled water) was incubated with a solution of 20 mM 2-iminothiolane (250 μL in distilled water) at a molar ratio of 20:1 (iminothiolane:dextran) for 60 min at room temperature. Unbound 2-iminothiolane was removed by dialysis using a Slide-A-Lyzer® MINI dialysis unit (7 kDa MWCO; obtained from Pierce) for 16 h. Next, a mixed solution (500 μL total volume) comprised of 0.5 mM thiolated dextran (250 μL in distilled water) and 0.1 mM *m*PEG-SH (250 μL in distilled water) was added to a solution of the 5-nm AuNPs (83 nM in 2.5 mL distilled water) to give a final molar ratio of AuNP:thiolated dextran:*m*PEG-SH ≈ 1:600:120. After gently stirring the mixture for 5 h under darkness at room temperature, free thiolated dextran and free *m*PEG-SH were removed from the AuNP conjugates by microfiltration (Microcon YM-50, 50 kDa MWCO, Millipore Corp.) and centrifugation (10,000 rpm for 15 min). The dextran-conjugated AuNPs were then resuspended in 50 mM HEPES buffer (pH 7.4) and used immediately for further experiments. The final concentration of the nanoparticles in solution was calculated using the molar extinction coefficient ($1.0 \times 10^7\ M^{-1}\ cm^{-1}$) for the 5-nm AuNPs at 513 nm.

2.3. Synthesis of ConA-QD

Carboxyl QDs (6.25 μL at 8 μM) and EDC (5 μL at 50 mM) were added to distilled water to give a final volume of 250 μL. The EDC-modified QDs were purified from excess EDC using a Microcon YM-50 centrifugal filter unit (50 kDa MWCO) and centrifugation (10,000 rpm for 15 min) followed by washing with distilled water. Upon redispersing the EDC-modified QDs in 200 μL HEPES buffer (50 mM, pH 7.4) a 40 μL solution of ConA (50 μM in 50 mM HEPES buffer, pH 7.4) was added. The resulting mixture was incubated for 60 min at room temperature. To block the remaining EDC-activated intermediate groups on the QD surface, a solution of *m*PEG-NH_2 (10 μL at 250 μM) was added, and the resulting mixture was further incubated for 30 min. The ConA-QD conjugates were purified from excess ConA and *m*PEG-NH_2 using microfiltration (300 kDa MWCO, Pall Filtron, Northborough, USA) and centrifugation (10,000 rpm for 20 min) followed by washing with distilled water three times. The purified conjugates were redispersed in 50 mM HEPES buffer (pH 7.4) and stored in darkness at 4 °C before use. The final concentration of the QDs (200 nM) was determined by measuring the absorbance of the solution at 488 nm and using molar extinction coefficients of $1.3 \times 10^5\ M^{-1}\ cm^{-1}$ (QD525) and $1.1 \times 10^6\ M^{-1}\ cm^{-1}$ (QD605) (from the manufacturer's specifications for the carboxyl QDs at 488 nm).

2.4. Synthesis of neoglycoproteins

For the synthesis of neoglycoproteins such as Man-BSA or Gal-BSA, a portion of the surface lysine residues of BSA were modified with α-D-mannopyranosyl phenyl isothiocyanate (MPI) through covalent bonding between isothiocyanate and ε-amine groups (Raja et al., 2003). An MPI stock solution was freshly prepared in DMSO, and the coupling reaction was carried out in 0.05 M sodium bicarbonate buffer (pH 9.0) containing 20% DMSO at 4 °C for 24 h. For the synthesis of BSA with different degrees of mannosylation, the molar ratio of MPI to BSA was varied from 1.5 to 150. The differently mannosylated BSA molecules (Man-BSAs) were analyzed to quantify the number of conjugated mannose units per BSA molecule by using BioLC DX-600 (Dionex, U.S.A.) chromatography, as mentioned earlier (Oh et al., 2006). The synthesis of Gal-BSA was performed by following the same general procedure using β-D-galactopyranosyl phenyl isothiocyanate (GPI). The resulting mixture was filtered and washed four times with 10 mM sodium bicarbonate buffer using a Microcon YM-10 centrifugal filter unit (10 kDa MWCO, Millipore Corp.) to remove the free MPI/GPI. For the determination of purity, the synthesized Man-BSA or Gal-BSA was subjected to carbohydrate analysis. Finally, the purified glycoproteins were resuspended in 10 mM sodium bicarbonate buffer and stored at −20 °C until further use.

2.5. PL quenching between Dex-AuNPs and ConA-QDs in solution

For the quenching experiments, ConA-QDs were mixed with varying amounts of either dextran-conjugated or free AuNPs in a 96-well microtiter plate for 1 h at room temperature. As an additional control, Alexa Fluor 647-labeled dextan was used as an acceptor. The final concentration of the QDs in aqueous solution was typically 10 nM (corresponding to 1 pmol QDs in a 100 μL reaction volume). Following the incubation period, the fluorescence was measured in a microplate reader (Infinite™ M200, TECAN, Austria) using an excitation wavelength of 605 nm. The mean and standard deviation of the fluorescence intensities were calculated from duplicate experiments. The quenching efficiency (Q_E) between donor and acceptor was determined by measuring the photoluminescence (PL) intensity of QDs in the presence and absence of energy acceptor (Eq. (1)).

2.6. On-chip detection of glycoprotein

For the chip-based analyses, a multiwell-type chambered silicon cover-slip (ϕ 3 mm × H 1 mm, Sigma) was overlaid onto an NHS-derivatized hydrogel glass slide (Schott Nexterion™, Germany). A solution (10 μL) containing 10 nM ConA-QDs in HEPES buffer (pH 7.4) was dropped into the wells formed by the chambered silicon cover-slip. The slide was incubated for 1 h at room temperature and the QD-immobilized wells then were immersed in a solution of 2% BSA (in 50 mM HEPES buffer) for 1 h to block the remaining NHS groups. After rinsing with distilled water, the wells were incubated either in a solution of Dex-AuNPs (10 μL at 100 nM) or in a mixture of Dex-AuNPs and glycoproteins (Man-BSA, Gal-BSA, or fetuin). Unless otherwise stated, the reaction solutions contained Ca^{2+}, Mn^{2+}, and Mg^{2+} at a final concentration of 100 μM to enhance the binding affinity between ConA and carbohydrate groups. Next, the slide was incubated for an additional 1 h at room temperature. The wells on the slide were then rinsed three times with distilled water and dried with a stream of nitrogen (N_2). An equal amount of BSA was used as another control. After measuring the PL intensity in each well, changes in energy transfer efficiency with respect to different concentrations of glycoprotein or varying numbers of mannose groups per BSA molecule were calculated along with the resulting IC_{50} values.

2.7. Fluorescence read-out

Fluorescence scanning was carried out by using an arrayWoRx^e slide scanner (Applied Precision, U.S.A.) equipped with a white-light CCD camera. For measurements of the PL intensity from different QDs, the glass slide was scanned using 525 nm (QD525) and 605 nm (QD605) emission filters (Chroma Tech. Corp., U.S.A.) with a common 460 nm (Chroma Tech. Corp., U.S.A.) excitation filter. After scanning, spot fluorescence intensities were analyzed by using imaging software (GenePix Pro 4.0, Axon), and the mean signal intensities and standard deviations of the respective spots were calculated from two independent experiments.

2.8. Calculations of quenching efficiency, normalized PL and IC_{50} values

The Förster distance (R_0) for the QD–AuNP system was estimated by using the Förster formula and by calculating the degree of spectral overlap between the donor QD emission spectrum and the absorbance spectrum of the acceptor AuNP as described elsewhere (Förster, 1948). We presumed that the quantum yield of the carboxyl QD605 particles and the refractive index of the biomolecules are 0.55 and 1.4 in aqueous solution, respectively. The orientation factor is further assumed to be 2/3. Given these parameter values and the overlap characteristics of the normalized donor emission and acceptor absorbance spectra, the Förster radius of the QD605-AuNP pair was calculated to be 6.2 nm.

The energy transfer between the QDs and AuNPs can be determined from the quenching efficiency (Q_E) of the experimentally obtained PL data. Considering multiple acceptors per QD, the overall efficiency can be represented as (Clapp et al., 2004):

$$Q_E = 1 - \frac{PL_{DA}}{PL_D} = \frac{nR_0^6}{nR_0^6 + r^6} \quad (1)$$

where PL_D is the PL intensity of the donor alone, PL_{DA} is the PL intensity of the donor in the presence of acceptor(s), r is the separation distance from the center of the QD to the acceptor, and n is the number of surface-bound acceptors.

With the experimentally determined value of Q_E, Eq. (1) can be rearranged to determine the D–A distance (r) using the value of R_0 calculated above:

$$r = \left(\frac{n(1 - Q_E)}{Q_E}\right)^{1/6} R_0 \quad (2)$$

For quantitative determinations of chip-based fluorescence, the normalized PL intensities are expressed as:

$$\text{normalized PL} = 100 \times \frac{PL_{Man-BSA} - PL_{BSA}}{(PL_{Man-BSA} - PL_{BSA})_{Max}} \quad (3)$$

where $PL_{Man\text{-}BSA}$ and PL_{BSA} represent the PL intensity between ConA-QDs and Dex-AuNPs after adding mannosylated BSA and native BSA, respectively. $PL_{Man\text{-}BSA} - PL_{BSA}$ indicates differences in the PL intensity between the mannosylated-BSA and native BSA. $(PL_{Man\text{-}BSA} - PL_{BSA})_{Max}$ indicates maximum differences in the PL intensity.

For determination of IC_{50} value, the normalized PL intensity data were plotted as a function of glycoprotein concentration and then fitted to a 4-parameter logistic equation by non-linear regression (SigmaPlot version 10.0, SYSTAT Software) using the following equation:

$$PL(\%) = \frac{PL_{max} - PL_{min}}{1 + (C/C_0)^n} + PL_{min} \quad (4)$$

where PL_{max} and PL_{min} indicate the maximum and minimum values of the normalized PL intensities, respectively; C_0 is the median concentration; C represents the concentration of glycoprotein; n is the slope factor. In graphical terms, the IC_{50} value is equal to the inflection point (C_0) of the best-fit curve.

3. Results and discussion

3.1. Chip-based detection of glycoprotein

Scheme 1 illustrates the detection principle. Lectin-conjugated QDs (Lec-QDs) are immobilized on an amine-reactive glass surface (NHS-hydrogel slide). The irradiation of light onto the backside of the glass surface results in a strong PL signal from the immobilized Lec-QDs (Scheme 1A). When in close proximity to these luminescent QDs, the carbohydrate-conjugated AuNPs (Carbo-AuNPs) function as a quencher due to the binding affinity between the lectin and carbohydrate groups (Scheme 1B). However, if glycoproteins are also present in the solution containing the Carbo-AuNPs (Scheme 1C) then the glycan moiety on the glycoproteins causes a reduction in energy transfer between the Lec-QDs and Carbo-AuNPs due to competitive inhibition, resulting in partial recovery of the PL of the QDs.

To examine the specificity of our detection system, non-glycoprotein and glycoprotein with different glycosylation degrees were compared as control and test samples, respectively (Fig. 1). As a proof-of-concept, concanavalin A-conjugated QDs (ConA-QDs) and dextran-modified AuNPs (Dex-AuNPs) were used as energy donors and acceptors, respectively. The carboxy QDs were conjugated with ConA by EDC modification, and the Dex-AuNPs were synthesized by conjugating a mixture of thiolated dextran and *m*PEG-SH with 5-nm AuNPs. Since dextran-ConA has a smaller binding affinity constant than mannosylated BSA-ConA, the addition of BSA conjugated with 22 mannose molecules (Man-BSA) led to a strong PL intensity, compared to the much weaker, quenched PL signal observed between the ConA-QDs and Dex-AuNPs. In contrast, strong PL intensities were not obtained when either carbohydrate-free BSA, galactose-modified BSA (Gal-BSA) or sialic acid-rich fetuin was added. These results indicate that the present assay system is

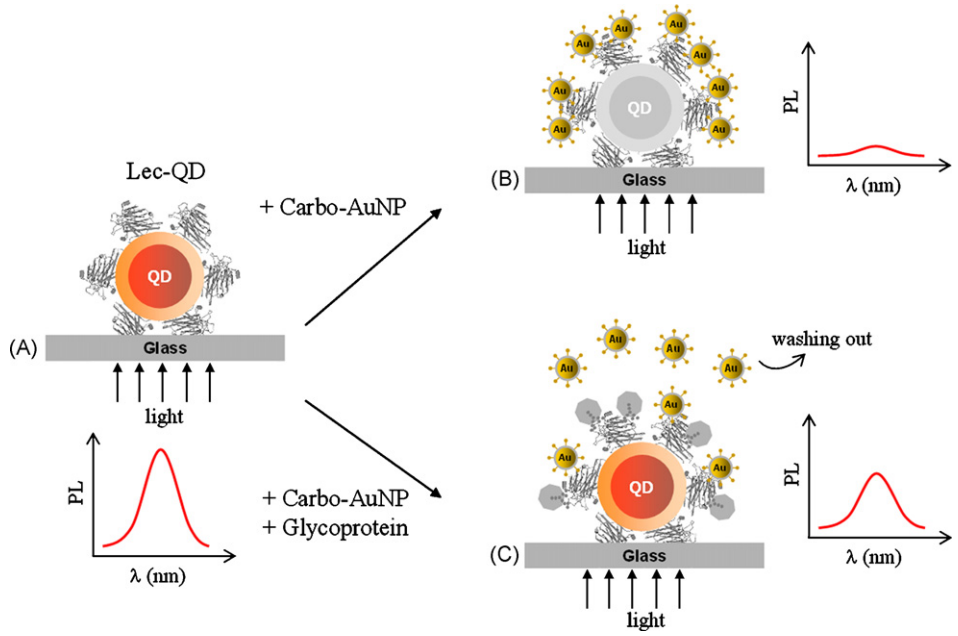

Scheme 1. Schematic principle for assay of the glycoprotein based on the energy transfer between lectin-modified QDs (Lec-QDs) and carbohydrate-conjugated AuNPs (Carbo-AuNP) on a glass slide.

specific for mannose-conjugated proteins. The inclusion of divalent ions (Ca^{2+}, Mn^{2+} and Mg^{2+}) in the reaction solution was found to increase the binding affinity between ConA-QD and Dex-AuNP, resulting in a higher degree of quenching and further improving the detection sensitivity for target glycoproteins (data not shown). The use of QDs with different colors (QD525 in Fig. 1A; QD605 in Fig. 1B) gave rise to similar changes in the PL intensity as a result of specific binding events. Based on these results, it seems clear that the Dex-AuNPs can be employed as common energy acceptor for different kinds of ConA-modified QDs, suggesting that this donor-acceptor system might be suitable for the development of a chip-based, multiplexed platform for the detection of glycoproteins.

3.2. Energy transfer between QDs and AuNPs

To obtain further insights into the energy transfer characteristics of our QD–AuNP system, we examined the degree of quenching as a function of the ratio of the acceptor-to-donor concentration. As shown in Fig. 2, increases in the quenching efficiency (Q_E) for the ConA-QDs were most significant when the Dex-AuNPs were used (Fig. 2A), but addition of unmodified AuNPs resulted in a modest increase in the quenching efficiency (Fig. 2B). The low Q_E values obtained for the carbohydrate-free AuNPs might be caused by a diffusion-driven quenching or non-specific binding of free AuNPs rather than an affinity-induced one. The quenching of QDs reached a maximum level at the molar ratio (10:1–20:1) of acceptor-to-donor (Fig. 2A). Further increase in the molar ratio resulted in a marginal enhancement of quenching efficiency (data not shown). The saturated molar ratio may represent the maximum binding number of Dex-AuNPs per single ConA-QD. The mean diameters of ConA and dextran were estimated to be 6–9 nm (based on considerations of the molecular dimensions of tetrameric ConA; 6.3 × 8.7 × 8.9 nm) (Hardman and Ainsworth, 1972) and 3 nm (based on a Strokes diameter of 10 kD for dextran), respectively. Accordingly, the distance from the surface of QDs to the surface of the AuNPs is expected to be 9–12 nm, which lies within the upper limit of the range of distances for FRET to occur. In

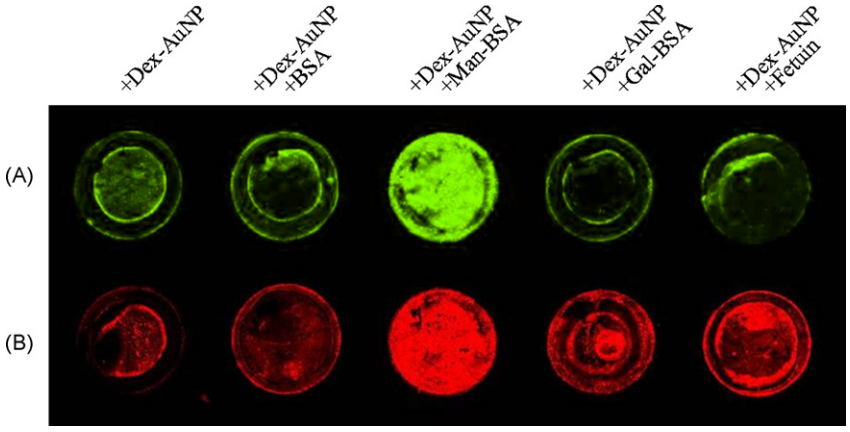

Fig. 1. On-chip detection of glycoproteins using concanavalin A-modified QDs (ConA-QDs) and dextran-conjugated AuNPs (Dex-AuNPs). The PL intensities of (A) ConA-QD525 and (B) ConA-QD605 were observed in the presence or absence of BSA, mannosylated BSA, galactosylated BSA, and fetuin. The concentrations of ConA-QDs, Dex-AuNPs and glycoproteins were 10, 100 and 500 nM, respectively.

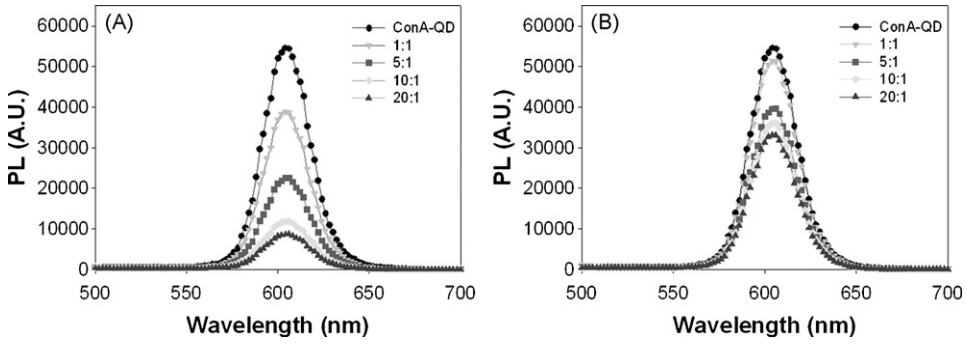

Fig. 2. Quenching effects of (A) Dex-AuNPs and (B) unmodified AuNPs on the PL of ConA-QDs in solution. The ratios of acceptor to donor were varied from 1:1 to 20:1 (from top to bottom). The concentration of ConA-QDs was held constant at 10 nM, and Ca^{2+}, Mn^{2+}, and Mg^{2+} (all at 100 μM) were added to the reaction buffer.

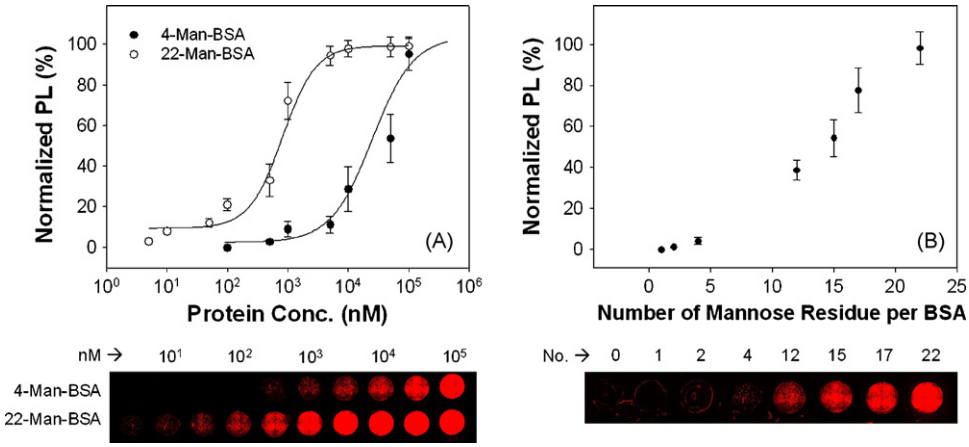

Fig. 3. Changes in the PL intensity for the ConA-QD and Dex-AuNP systems as a function of either (A) the concentration of mannosylated BSA (5-Man-BSA and 22-Man-BSA) or (B) the number of conjugated mannose residues per BSA molecule. Error bars indicate the standard deviation derived from duplicate experiments.

contrast to the QD605-Alexa647 pair, the energy transfer characteristics of the QD605-AuNP system showed a higher quenching efficiency and a shorter separation distance of 7.4 nm than the estimated one (9.0–12.0 nm) of surface-to-surface between QD and AuNP (Table 1). Two acceptors, dextran-conjugated Alexa647 (Dex-Alexa647) and Dex-AuNP, are different in their sizes. Typically, Dex-AuNP (multi-binding of dextran per AuNP) is much larger than Dex-Alexa647 (1:1 binding) and, it might have less binding number than the Dex-Alexa647 at a similar ratio of donor-to-acceptor. Nonetheless, high quenching efficiency and short distance for QDs/AuNPs might result from different energy transfer mechanism from conventional FRET. The strong quenching ability of the AuNPs combined with their high capacity for multiple binding as shown in Fig. 2A might be allowing the present energy transfer system to become effective beyond the traditional FRET distance. Indeed, it is noteworthy that the use of AuNPs as an energy acceptor has previously been shown by others to extend the effective energy transfer distance up to 22 nm, resulting in a high energy transfer efficiency (Yun et al., 2005).

Table 1
Comparison of the energy transfer characteristics for ConA-QD (donor) and Dex-AuNPs or Dex-Alexa Fluor 647 (acceptors) in solution

Donor/acceptor	Expected distance (nm)[a]	R_0 (nm)[b]	Q_E (%)[c] (n = 10)	r (nm)[d]
ConA-QD605/Dex-AuNP	9.0–12.0	6.2	78.2	7.4
ConA-QD605/Dex-Alexa647	9.0–12.0	6.8	35.4	11.0

[a] These values refer to the expected distance from the surface of the donor to the surface of the acceptor, taking into account the sizes of ConA and dextran.
[b] The Förster distance (R_0) values for the QD-AuNP and QD-Alexa647 pairs were calculated in Section 2.
[c] The quenching efficiency (Q_E) was calculated from Eq. (1).
[d] The separation distance (r) was determined according to Eq. (2).

Size-tunable QDs have different geometry and diameter (QD525 and QD605 in this study), which can result in different binding numbers of lectin molecule on the surface of QD. However, the size of QDs can affect only the quenching state of QD, due to the different binding numbers of acceptor. Since detection of glycoprotein, which is typically compared with the control group without glycan moiety, was conducted using the same QDs, we could minimize the size effect of QD on analysis of glycoproteins.

3.3. Quantitative analysis of glycoprotein on a surface

We further attempted to quantify the glycoproteins in terms of their concentration and the number of glycan moieties per BSA molecule. The PL difference between native BSA and Man-BSA was normalized to the maximum PL difference at excess protein concentration (Eq. (3)), and the concentration-dependent IC_{50} values were calculated from Eq. (4). By examining the changes in the PL emission properties of the QD–AuNP system as a function of varying concentrations of Man-BSA, the IC_{50} values for 5-Man-BSA (BSA with 5 mannose molecules), and 22-Man-BSA (BSA with 22 mannoses) were estimated to be 39 μM and 820 nM, respectively (Fig. 3A). The difference in the IC_{50} values indicates that 22-Man-BSA, which contains a higher degree of mannosylation, induced a stronger level of competitive inhibition in the energy transfer system, when compared to 5-Man-BSA. The detection limit for the 22-Man-BSA glycoprotein was 10 nM, which is much lower than the

limit values that have been achieved using other methods (Blagoi et al., 2005; Mislovicova et al., 2002) and is comparable with the value previously reported by using a solution-based method (Oh et al., 2006). The linear detection ranges for 4-Man-BSA and 22-Man-BSA were estimated to be 5×10^3 to 10^5 and 10^2 to 10^4 nM, respectively. These ranges were slightly narrower than that reported previously (Sezginturk and Dinckaya, 2008). However, in the case of glycoprotein, the average glycan number of target molecule should be considered in evaluation of the linear detection range, because the glycan number is closely linked to binding affinity, which leads to a change in the detection range. When the change in signal intensity was measured with respect to the glycan number, the PL emission of the ConA-QD was found to increase linearly with increasing numbers of mannose residues conjugated to BSA (Fig. 3B). Based on these results, our system is expected to be effective for quantitative analyses of the degree of protein glycosylation.

Various chip-based methods to analyse glycoproteins (carbohydrate chip, lectin-based chip, or peptide-aptamer chip, *etc.*) have been attempted and higher detection sensitivity has been reported. However, compared to these chip-based systems employing a single fluorophore-based intensity, our system offers several advantages; photobleaching and background noise were significantly reduced. An electrochemical method (Sadik and Yan, 2007) can offer more convenient procedure than other systems in terms of measuring time and simplicity, but it has still limitations in a high-throughput or multiplexed assay. For the development of a high-throughput format based on electrochemistry, a microfluidic device is required. In this case, high voltage field interference and biofouling on electrode can be an issue, and these often cause a reduction in sensitivity. Parallel with the electrochemical method, fluorescence-based techniques have been extensively developed on current biochip field. In this regard, the QD/AuNP-based energy transfer system has a high potential for a multiplexed and high-throughput analysis in fluorescence-based area. In particular, nanoparticle-based biochip system is on the demand of advanced technologies even though some issues still remain challenging. We anticipated that further optimization of the assay system will improve the detection sensitivity and consequently our system will find application in the glycomics field.

4. Conclusions

In conclusion, we have demonstrated that a chip-based detection system relying on the energy transfer between biofunctionalized QDs and AuNPs enabled a rapid and sensitive analysis of protein glycosylation with a high degree of reliability and with no aggregation of the nanoparticles. Furthermore, the AuNPs could be employed as energy acceptors in conjunction with QDs with differing colors, suggesting that it would be possible to develop a multiplexed assay of glycoproteins using various combinations of lectins and carbohydrate ligands. It is expected that our assay system will find broad applications in the analysis of glycoproteins in a high-throughput manner.

Acknowledgements

This work was supported by the Nano-Science & Technology Program (M10503000868-07M0300-86810) the Nano/Bio Science & Technology Program (M10536090002-08N3609-00210) and the Brain Korea 21 Program of MEST, the Korea Health 21C R&D Project (0405-MN01-0604-0007) of MIHWAF, and the Next-Generation New-Technology Development Program for MKE.

References

Bertozzi, C.R., Kiessling, L.L., 2001. Science 291 (5512), 2357–2364.
Blagoi, G., Rosenzweig, N., Rosenzweig, Z., 2005. Anal. Chem. 77 (2), 393–399.
Caron, M., Seve, A.P., Bladier, D., Joubert-Caron, R., 1998. J. Chromatogr. B. Biomed. Sci. Appl. 715 (1), 153–161.
Chen, S., LaRoche, T., Hamelinck, D., Bergsma, D., Brenner, D., Simeone, D., Brand, R.E., Haab, B.B., 2007. Nat. Methods 4 (5), 437–444.
Clapp, A.R., Medintz, I.L., Mauro, J.M., Fisher, B.R., Bawendi, M.G., Mattoussi, H., 2004. J. Am. Chem. Soc. 126 (1), 301–310.
Förster, T., 1948. Ann. Phys. Med. 2, 55–75.
Hardman, K.D., Ainsworth, C.F., 1972. Biochemistry 11 (26), 4910–4919.
Kim, M., Han, S.H., Shin, Y.-B., Chung, B.H., 2007a. Biochip J. 1 (2), 81–89.
Kim, Y.-P., Oh, Y.-H., Oh, E., Kim, H.-S., 2007b. Biochip J. 1 (4), 228–233.
Kim, Y.-P., Oh, Y.-H., Oh, E., Ko, S., Han, M.-K., Kim, H.-S., 2008. Anal. Chem. 80 (12), 4634–4641.
Manimala, J.C., Roach, T.A., Li, Z., Gildersleeve, J.C., 2006. Angew. Chem. Int. Ed. Engl. 45 (22), 3607–3610.
Mann, D.A., Kanai, M., Maly, D.J., Kiessling, L.L., 1998. J. Am. Chem. Soc. 120 (41), 10575–10582.
Medintz, I.L., Clapp, A.R., Mattoussi, H., Goldman, E.R., Fisher, B., Mauro, J.M., 2003. Nat. Mater. 2 (9), 630–638.
Mislovicova, D., Masarova, J., Svitel, J., Mendichi, R., Soltes, L., Gemeiner, P., Danielsson, B., 2002. Bioconjug. Chem. 13 (1), 136–142.
Oh, E., Hong, M.Y., Lee, D., Nam, S.H., Yoon, H.C., Kim, H.S., 2005. J. Am. Chem. Soc. 127 (10), 3270–3271.
Oh, E., Lee, D., Kim, Y.P., Cha, S.Y., Oh, D.B., Kang, H.A., Kim, J., Kim, H.S., 2006. Angew. Chem. Int. Ed. Engl. 45 (47), 7959–7963.
Ohtsubo, K., Marth, J.D., 2006. Cell 126 (5), 855–867.
Pilobello, K.T., Krishnamoorthy, L., Slawek, D., Mahal, L.K., 2005. Chembiochem 6 (6), 985–989.
Raja, K.S., Wang, Q., Finn, M.G., 2003. Chembiochem 4 (12), 1348–1351.
Sadik, O.A., Yan, F., 2007. Anal. Chim. Acta 588 (2), 292–296.
Sapsford, K.E., Berti, L., Medintz, I.L., 2006. Angew. Chem. Int. Ed. Engl. 45 (28), 4562–4589.
Sezginturk, M.K., Dinckaya, E., 2008. Biosens. Bioelectron. 23 (12), 1799–1804.
Yun, C.S., Javier, A., Jennings, T., Fisher, M., Hira, S., Peterson, S., Hopkins, B., Reich, N.O., Strouse, G.F., 2005. J. Am. Chem. Soc. 127 (9), 3115–3119.
Zamfir, A., Peter-Katalinic, J., 2004. Electrophoresis 25 (13), 1949–1963.
Zhang, J., Badugu, R., Lakowicz, J.R., 2008. Plasmonics 3, 3–11.